Chemical assembly of multiple metal cofactors: The heterologously expressed multidomain [FeFe]-hydrogenase from Megasphaera elsdenii.

Georgio Caserta, Agnieszka Adamska-Venkatesh, Ludovic Pecqueur, Mohamed Atta, Artero Vincent, Souvik Roy, Edward Reijerse, Wolfgang Lubitz, Marc Fontecave

Chemical assembly of multiple metal cofactors: the heterologously expressed multidomain [FeFe]-hydrogenase from *Megasphaera elsdenii*.

Giorgio Caserta[a], *Agnieszka Adamska-Venkatesh*[b], *Ludovic Pecqueur*[a], *Mohamed Atta*[c], *Vincent Artero*[c], *Roy Souvik*[c], *Edward Reijerse*[b], *Wolfgang Lubitz*[b] *and Marc Fontecave*[a]*

[a] Laboratoire de Chimie des Processus Biologiques, Collège de France,
Université Pierre et Marie Curie, CNRS UMR 8229, 11 place Marcelin Berthelot,
75005 Paris, France

[b] Max-Planck-Institut für Chemische Energiekonversion, Stiftstrasse 34-36,
45470 Mülheim an der Ruhr, Germany.

[c] Laboratoire de Chimie et Biologie des Métaux, Université Grenoble Alpes, CEA/BIG,
CNRS, 17 rue des martyrs, 38000 Grenoble, France

* to whom correspondence should be addressed : mfontecave@cea.fr; tel : (33) 144271360

ABSTRACT

[FeFe]-hydrogenases are unique and fascinating enzymes catalyzing the reversible reduction of protons into hydrogen. These metalloenzymes display extremely large catalytic reaction rates at very low overpotential values and are, therefore, studied as potential catalysts for bioelectrodes of electrolyzers and fuel cells. Since they contain multiple metal cofactors whose biosynthesis depends on complex protein machineries, their preparation is difficult. As a consequence still few have been purified to homogeneity allowing spectroscopic and structural characterization. As part of a program aiming at getting easy access to new hydrogenases we report here a methodology based on a purely chemical assembly of their metal cofactors. This methodology is applied to the preparation and characterization of the hydrogenase from the fermentative anaerobic rumen bacterium *Megasphaera elsdenii*, which has only been incompletely characterized in the past.

Keywords : [FeFe]-hydrogenase, *Megasphaera elsdenii*, synthetic maturation, H_2 production

ABBREVIATIONS

β-met, β-mercaptoethanol; DTT, dithiothreitol; adt, azadithiolate; DMSO, dimethylsulfoxide; EPR, electron paramagnetic resonance; FTIR, Fourier transform infrared; TOF, turnover frequency; Tris, tris(hydroxymethyl)-aminomethane; GC, Gas chromatography; SEC, size exclusion chromatography; MeHydA, [FeFe]-hydrogenase from *Megasphaera elsdnii*; CrHydA1, [FeFe]-hydrogenase from *Chlamydomonas reinhardtii*; CpHydA, [FeFe]-hydrogenase from *Clostridium pasteurianum*; DdH, [FeFe]-hydrogenase from *Desulfovibrio desulfuricans*; CaHydA, [FeFe]-hydrogenase from *Clostridium acetobutylicum*; apo-MeHydA, MeHydA

without FeS cluters; FeS-MeHydA, MeHydA reconstituted with [4Fe4S] clusters; Holo-MeHydA, FeS-MeHydA maturated with $[Fe_2(adt)(CO)_4(CN)_2]^{2-}$; H_{ox}, oxidized state of [FeFe]-hydrogenase; H_{ox}-CO, CO-inhibited oxidized state of [FeFe]-hydrogenase; H_{red}, reduced state of [FeFe]-hydrogenase; H_{sred}, superreduced state of [FeFe]-hydrogenase; CW, Continuous Wave; FID, Free Induction Decay.

1. Introduction

[FeFe]-hydrogenases, named HydA, are unique biocatalysts for the interconversion between protons and dihydrogen[1]. These metalloenzymes display extremely large catalytic reaction rates at very low overpotential. As a consequence, they have been well studied from structural and mechanistic perspectives [2–4]. Furthermore they are considered as potential alternative catalysts to noble metals for the development of novel bio-fuel cells and bio-electrolyzers as well as bio-photoelectrochemical cells [5–8]. These green technological electrochemical devices might contribute to solve the energy storage issue linked to the intermittency of renewable energies such as solar and wind energies. A large number of studies have thus been devoted to the investigation of the electrochemical behavior of these enzymes at carbon-based surfaces as well as in combination with semiconducting materials in order to optimize bio-electrodes or bio-photoelectrodes [9,10]. These enzymes display remarkable electrocatalytic activity for proton reduction into H_2 but also suffer from extreme oxygen sensitivity [11–15]. Finally, spectroscopic and structural studies provide a knowledge that is extensively exploited by synthetic chemists for the preparation and development of bioinspired catalysts, mimicking the unique diiron active center of these enzymes [16,17].

[FeFe]-hydrogenases indeed rely, for activity, on a complex inorganic site, consisting of an organometallic dinuclear Fe subunit, named 2Fe-subcluster, in which the two Fe atoms are bridged by an aza-propanedithiolate (adt^{2-}) ligand and the coordination sphere is completed by CO and cyanide ligands [18]. This diiron complex is linked to a [4Fe-4S] cluster via a sulfur atom of a cysteine residue. This active site, thus containing 6 Fe atoms and named the "H-cluster", is buried inside the protein but is connected to the surface of the protein, for electron transfer, in most cases via an array of iron-sulfur [FeS] clusters (Figure 1). Interestingly, the number of accessory [FeS] clusters varies from one enzyme to another. For example, HydA from *Clostridium pasteurianum* [19,20] contains one [2Fe-2S] and three [4Fe-4S] clusters, HydA from *Desulfovibrio desulfuricans* [21] harbors two [4Fe-4S] clusters while HydA from the green algae *Chlamydomonas reinhardtii* [22] has no accessory [FeS] clusters.

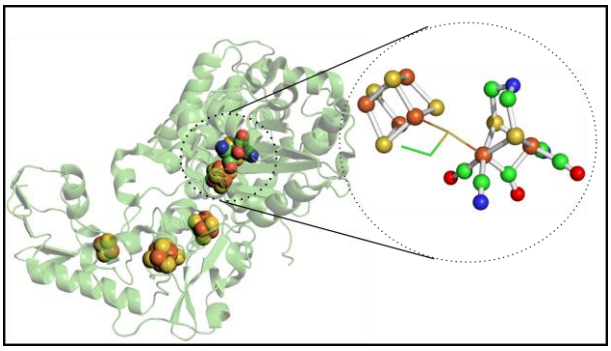

Figure 1. X ray structure of CpHydA with its protein surrounding, PDB 4XDC [28]. CpHydA has 1 [2Fe2S], 2 [4Fe4S] clusters and the H-cluster depicted in the circle. The picture is designed using the program PYMOL. Fe atoms are depicted in brown, S in yellow, C in green, N in blue and O in red.

Biomolecular studies on [FeFe]-hydrogenases are unfortunately limited by the fact that these enzymes are difficult to prepare. First, they have to be purified and manipulated only under strict anaerobiosis. Second, their maturation, the process by which the [FeS] clusters and the 2Fe-subcluster are synthesized and assembled, depends on complex and specific protein

machineries. In particular, the system involved in the biosynthesis of the 2Fe-subcluster is still incompletely characterized [23]. Three enzymes are participating in the biosynthetic pathway. HydG and HydE are S-adenosyl-L-methionine enzymes. HydG has been shown to produce an {Fe-$(CO)_2(CN)$} synthon that is the first intermediate towards the 2Fe-subcluster [24]. HydE is proposed to participate in the synthesis of the adt^{2-} ligand through an as yet unknown mechanism. HydF, is a GTPase that binds a [4Fe-4S] cluster and serves as a scaffold/carrier protein for assembly of a precursor of the 2Fe-subcluster of HydA. Transfer of the latter to HydA, containing the [Fe-S] clusters but lacking the 2Fe-subcluster, produces a fully active hydrogenase. The three proteins are absent from *Escherichia coli* which is the bacterial expressing system, very widely used for recombinant protein preparation [1,25]. As a consequence few [FeFe]-hydrogenases have been purified to homogeneity and only three have been structurally characterized [19–22]. There is thus a need to get easier access to more members of that class of enzymes.

Recently, we discovered that recombinant [FeFe]-hydrogenases can be prepared anaerobically in an inactive form containing only the [FeS] clusters and subsequently fully maturated by reaction with the synthetic $[Fe_2(adt)(CO)_4(CN)_2]^{2-}$ biomimetic complex [26,27]. The resulting active site has been shown to display EPR and FTIR characteristics identical to those of the naturally maturated enzyme, as illustrated in the case of CrHydA1 from *Chlamydomonas reinhardtii*. In case of HydA from *Clostridium pasteurianum* the definitive confirmation that the chemically synthesized active site was identical to the biosynthesized one came from the observation of a remarkable identity of the two three-dimensional structures [28]. This synthetic maturation methodology has already led to a number of very interesting

applications which would have been otherwise unreachable, such as specific labeling of the active site or preparation of artificial hydrogenases [4,29–33].

Here, we go a step further towards the facile preparation of active hydrogenases in large amounts from standard *E. coli* strains lacking the HydEFG machinery. We show that it is sufficient to express the corresponding gene in *E. coli*, purify the apoprotein aerobically and activate it chemically, simply via, first, incorporation of the [FeS] clusters by treatment with iron and sulfide and, second, incorporation of the 2Fe-subunit by reaction with the $[Fe_2(adt)(CO)_4(CN)_2]^{2-}$ complex, anaerobically. This methodology is illustrated here with the preparation of HydA from the fermentative anaerobic rumen bacterium *Megasphaera elsdenii*. This enzyme, named MeHydA hereafter, has been previously isolated from a *M. elsdenii* strain but only partially characterized in the 1980's, when the structure of these enzymes was not yet known [34–37]. In this report, we provide a straightforward method for preparing a highly active hydrogenase. Furthermore we provide the first full characterization of MeHydA using EPR and FTIR spectroscopy.

Finally, up to now only two [FeFe] hydrogenases, HydA from *Desulfovibrio desulfuricans* (DdH) and from *C. reinhardtii* (CrHydA1), have been thoroughly studied for their redox behavior [38–40]. The observed redox states differ from each other substantially. The bacterial enzyme DdH can be prepared under aerobic conditions and isolated in the inactive air-stable H_{ox}^{air} state. Reductive activation leads to an intermediate redox state H_{trans} which converts into the active oxidized state called H_{ox}. While the H_{ox}^{air} and H_{trans} are not observed in any other [FeFe] hydrogenase, the H_{ox} state and its CO inhibited version H_{ox}-CO are found in all [FeFe] hydrogenases (Table 2). One electron reduction of H_{ox} (-400 mV NHE, pH 8.0) provides the reduced state H_{red}. Further reduction of DdH (-560 mV NHE, pH 8.0) is incomplete and leads

irreversibly to a weakly populated so called "super-reduced" H_{sred} state [38]. In contrast, in CrHydA1, lacking accessory [FeS] clusters, reduction to the super-reduced state (-460 mV NHE, pH 8.0) is complete and reversible [39,40]. In the current study, we also report, for the first time, the redox behavior of MeHydA.

2. MATERIALS AND METHODS

2.1. Expression and purification of apo-MeHydA

TunerDE3pLysS cells transformed with the pT7-7-6HMeHydA plasmid [41] were grown in Terrific Broth medium supplemented with ampicillin and chloramphenicol at 37 °C, until the optical density at 600 nm reached 0.5. Protein synthesis was induced by the addition of isopropyl β-D-thiogalactopyranoside to a final concentration of 0.5 mM. Cells were grown for an additional 5 h with decreasing the temperature to 20 °C to avoid the formation of inclusion bodies. Cells were harvested by centrifugation and stored at -80°C until use. Cells were resuspended in Tris Buffer 50 mM pH 8.0 containing 5 % v/v glycerol, 1 % v/v Triton, 1 mM Dithiothreitol (DTT) and 5mM β-Mercaptoethanol (β-met) and discontinuously sonicated for 10-12 min. Cellular extracts were centrifuged 1h at 193 000 g leading to a soluble fraction of HydA.

The first chromatographic step was performed on a His Trap column (GE-healthcare) equilibrated with 50 mM Tris-Cl pH 8.0, 300 mM NaCl, 10 % v/v glycerol, 5 mM β-met, 1 mM DTT. After loading, the column was extensively washed with 10 column volumes of 50 mM Tris-HCl pH 8.0, 300 mM NaCl, 10 % v/v glycerol, 5 mM β-met, 1 mM DTT, 10 mM imidazole then eluted with a linear gradient of buffer A/buffer A supplemented with 500 mM imidazole. Elution fractions containing 6H-MeHydA were pooled and a pure and homogeneous protein was obtained after a gel filtration step with a Superdex S200 26-600 equilibrated in 50 mM Tris-HCl

pH 8.0, 300 mM NaCl, 10 % glycerol, 5mM DTT. Protein concentrations were determined with the Bradford assay (Bio-Rad), using bovine serum albumin as a standard. The oligomeric state of the apo- and reconstituted proteins was determined in anaerobiosis via analytical gel filtration using a Superdex S200 10/300 column equilibrated in 50 mM Tris-HCl buffer pH 8.0, 300 mM NaCl, 10% v/v glycerol, 5 mM DTT. To estimate the molecular weight of apo-MeHydA, static light scattering measurements were performed in batch mode in a quartz cuvette on a Zetasizer ZSP (Malvern) using toluene as a standard. The measurements were done from apo-MeHydA freshly purified on a S200 10/300 GL column. The protein concentration was estimated with the Bradford assay. A dn/dc of 0.187 at 633 nm, calculated from the protein sequence using the program SEDFIT was used [42]. The molecular weight was extracted from the intercept of the linear fit with the Zimm equation for an isotropic scatterer, $Kc/R_\theta = 1/M + 2A_2c$, of the Debye Plot. K is an optical constant, c is the concentration of the analyte, R_θ is the Rayleigh ratio, M is the molecular weight and A_2 the second virial coefficient.

2.2. In vitro [4Fe-4S] clusters reconstitution of apo-MeHydA

[4Fe-4S] clusters reconstitution of apo-MeHydA was conducted under strictly anaerobic conditions in a glove box (MBraun) with less than 0.5 ppm O_2. After incubation of apo-MeHydA (50-100 µM) with 10 mM DTT for 15 min at 20°C, a 17-18 molar excess of ferrous ammonium sulfate [$(NH_4)_2Fe(SO_4)_2,6H_2O$] was added, followed by the addition of a 17-18 molar excess of L-cysteine and a catalytic amount of the *E. coli* cysteine desulfurase CsdA [43] (1–2 % molar equivalent). The reaction was monitored by recording UV–Visible absorption spectra every 30 min. For practical reason, [4Fe-4S] clusters reconstitution was performed overnight. The reconstituted FeS-MeHydA was then centrifuged 20 min at 12 000 rpm and purified on Superdex S200 10/300 GL equilibrated with the reconstitution buffer (50 mM Tris-HCl pH 8.0, 300 mM

NaCl, 10% Glycerol, 5 mM DTT). The pure FeS-MeHydA was concentrated with Amicon Ultra 30-kDa centrifugal filters (Millipore) and stored in liquid nitrogen or at -80 °C in sealed vials until use. Visible absorption spectra were recorded on a Cary 100 spectrophotometer (Agilent) connected to the cell holder located in a glovebox with optical fibers. For each sample, the Fe and S content was determined 3 times for 2 different protein concentrations according to the methods of Fish [44] and Beinert [45], respectively.

2.3. Synthesis of $(Et_4N)_2[Fe_2(adt)(CO)_4(CN)_2]$

$(Et_4N)_2[Fe_2(adt)(CO)_4(CN)_2]$, was prepared as previously described [27,46].

2.4. In vitro maturation of FeS-MeHydA for FTIR and EPR measurements

$(Et_4N)_2[Fe_2(adt)(CO)_4(CN)_2]$ was dissolved at a concentration of 80 mM in DMSO, and stored anaerobically at -80°C in sealed vials. In a standard experiment 50 µM FeS-MeHydA were incubated for 1h with 10 equivalents of $[Fe_2(adt)(CO)_4(CN)_2]^{2-}$in the maturation buffer at room temperature (100 mM potassium phosphate pH 6.8). The excess of $[Fe_2(adt)(CO)_4(CN)_2]^{2-}$ was removed by a desalting column (NAP-10, GE healthcare) and the protein was concentrated to 0.5−1 mM and stored in liquid N_2 or directly used for experiments. For activity experiments, the concentrated holo-MeHydA was diluted to 2-3 µM.

2.5. In vitro maturation of FeS-MeHydA for H_2 production

H_2 production was determined according to published procedure [26] by using methyl viologen as electron mediator and sodium dithionite as reducing agent. Briefly, holo-MeHydA (5−10 µL) corresponding to 20 pmol of hydrogenase was added to a total amount of 1.11 mL of 100 mM potassium phosphate, pH 6.8, 100 mM sodium dithionite, and 10 mM methyl viologen in a 10

mL vial sealed under anaerobic conditions (rubber stoppers, Carl Roth). In a second test a 10-fold excess of synthetic complex was added to monomeric FeS-MeHydA (2-3 µM), the mixture was incubated for 1 h at room temperature and the samples were used immediately for activity tests, as described above. A gas chromatogram was recorded on a GC System (Shimadzu GC-2014 with a thermal conductivity detector and a Quadrex column) and the amount of H_2 was quantified using a calibration curve. $[Fe_2(adt)(CO)_4(CN)_2]^{2-}$ and FeS-MeHydA were assayed as controls and did not show any activity. All activities in this study were measured at least 3 times on 3 different protein preparations.

2.6. FTIR and EPR analysis: isolation of H_{ox}, H_{red} and H_{ox}-CO states.

After FeS-MeHydA maturation with $(Et_4N)_2[Fe_2(adt)(CO)_4(CN)_2]$, an aliquot of the holoenzyme was flushed for 20 min with carbon monoxide to obtain H_{ox}-CO. In the same way, 1 aliquot of holo-MeHydA was flushed for 1h with Argon to isolate the H_{ox} state. To produce the Hred state presented in figure 3, 1 aliquot of the holoenzyme was flushed with H_2 for 24 h and subsequently treated with different concentration of sodium dithionite. For the progressive reduction series presented in figure S4, 80 µl of 0.5 mM enzyme were used. For each measurement a 10 µl sample was used.

Fourier Transform Infrared (FTIR) measurements were carried out using a Bruker IFS 66v/s FTIR spectrometer equipped with a nitrogen cooled Bruker mercury cadmium telluride (MCT) detector. The spectra were accumulated in the double-sided, forward-backward mode with 1000 scans (14 minutes total) and a resolution of 2 cm^{-1} at 15 °C. The obtained interferograms were automatically processed by the Opus software utilizing a 32-points phase correction and a Blackman–Harris 3-term apodization window. Baseline correction was done using a cubic spline

data interpolation procedure applied to manually selected points of the experimental spectra. Data processing was facilitated by home written routines in the MATLAB™ programming environment.

Q-band EPR spectra were recorded using free induction decay (FID) detected EPR with a microwave pulse length of 1 μs. All pulse experiments were performed on a Bruker ELEXYS E580 Q-band spectrometer with a SuperQ-FT microwave bridge and home built resonator described earlier [47]. Cryogenic temperatures (10-20 K) were obtained by an Oxford CF935 flow cryostat. For the interpretation of all EPR experimental data, a home written simulation program (based on the EasySpin package [48]) in MATLAB™ was used.

3. RESULTS AND DISCUSSION

3.1 Purification of the MeHydA and iron-sulfur clusters reconstitution.

Expression of the MeHydA-encoding gene in *E. coli* resulted in a large production of soluble recombinant protein. As the protein is His-tagged, it could be purified to homogeneity with only two chromatographic steps (Figures S1). After a His tag affinity column and a gel filtration step using a Superdex S200 chromatographic column the protein was purified to homogeneity and was finally concentrated to 5-7 mg/ml. Overall 10-15 mg of MeHydA could be obtained from 1 L of culture. All the purification procedures were carried out aerobically. β-mercaptoethanol and dithiothreitol (DTT) were needed in the buffers in order to limit the formation of oligomers, certainly via disulfide bridge reduction. While a very small amount of iron was detected in this preparation the protein was mainly in the apo form and was named apo-MeHydA. To incorporate the iron-sulfur clusters in apo-MeHydA, a standard protocol was used, consisting of the anaerobic incubation of the protein with an excess of iron ammonium sulfate

and cysteine in the presence of DTT. The reaction was initiated by addition of catalytic amounts of CsdA, a cysteine desulfurase, and monitored by light absorption spectroscopy since [FeS] clusters display a characteristic charge-transfer absorption band at 410 nm (Figure 2A and S2). Gel filtration provided evidence for the formation of large oligomers (Figure S3A), which were shown to be enzymatically inactive. Only the low-molecular weight protein fraction was collected and further characterized. While the elution volume of apo-MeHydA (13.7 mL) and reconstituted MeHydA (named FeS-MeHydA, 14.7 mL) were different (Figure S3B), both were shown to be monomers by static light scattering in batch mode to assess molecular weights using the Zimm equation and the Debye plot (Figure S3D). As a consequence, after [FeS] cluster reconstitution of MeHydA, the elution volume increased due to a change of the conformation of the protein, likely becoming more compact.

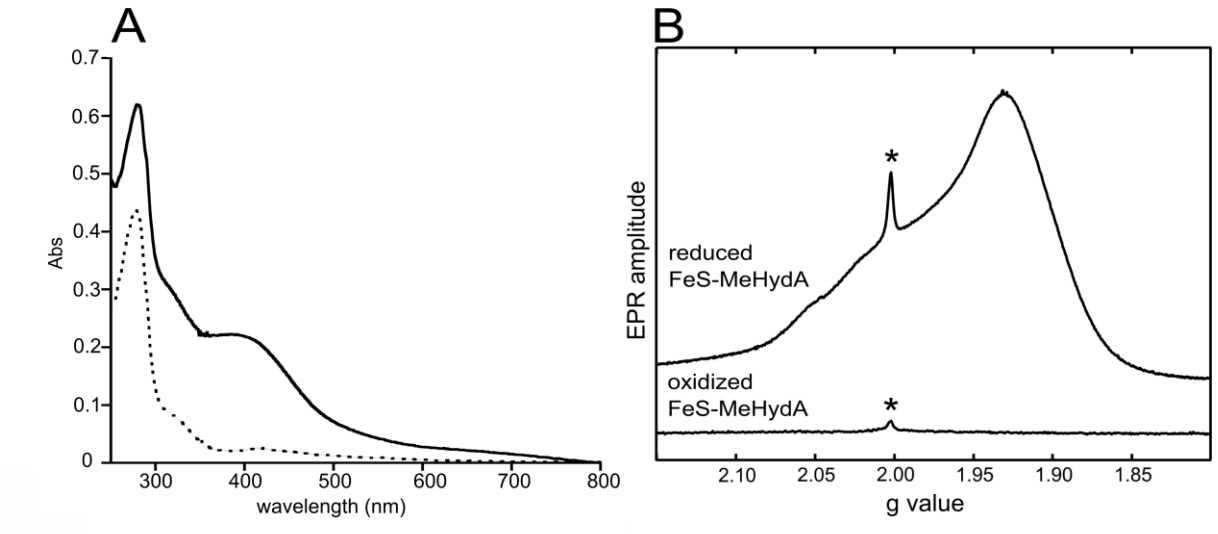

Figure 2. Spectroscopic characterization of reconstituted FeS-MeHydA. A) UV-visible spectra of 68 µM apo-MeHydA (dashed line) and FeS-MeHydA (solid line) in 50 mM Tris pH 8.0, 300 mM NaCl, 10% v/v glycerol, 5 mM DTT. B) Q-band FID-detected EPR spectra (10K) of 170 µM FeS-MeHydA, before (20K) and after (10K) reduction with sodium dithionite, in 50mM Tris pH 8.0, 300 mM NaCl, 10% v/v glycerol, 5 mM DTT. The g values obtained from a simulation (2.055, 1.930, 1.885) are typical for $[4Fe\text{-}4S]^{1+}$ clusters. The sharp signal at $g \approx 2.0$

marked with an asterisk is due to a radical originating from the aerobic purification of apo-MeHydA in the presence of DTT **[49]**.

The quantitation of Fe (10.5 ± 0.2 per protein) and S (11.0 ± 0.2 per protein) as well as the UV-Visible spectrum (Figure 2A) of the protein were in good agreement with the expected presence of three [4Fe-4S] clusters within a single polypeptide chain. To our knowledge it is the first time that this procedure proves effective for full reconstitution of three [4Fe-4S] clusters within a single polypeptide chain. The type of clusters present in the protein was further confirmed by Q-band EPR spectroscopy (Figure 2B). The reconstituted oxidized protein was EPR silent. However, upon anaerobic reduction using sodium dithionite, it became EPR active with overlapping signals characteristic of reduced S=1/2 $[4Fe\text{-}4S]^{+}$ clusters (Figure 2B). The spectrum does not indicate clear spin coupling (dipolar splitting) between the clusters as is observed in DdH [50] suggesting a slightly longer distance between them. These data show that the reconstitution process leads exclusively to S=0 $[4Fe\text{-}4S]^{2+}$ oxidized clusters and exclude the presence of $[3Fe\text{-}4S]^{+}$ and $[2Fe\text{-}2S]^{2+}$clusters. FeS-MeHydA is an interesting novel form of *M. elsdenii* HydA as it may allow studying the electron-transfer chain specifically.

MeHydA indeed contains, in addition to the H-cluster, two additional [FeS] clusters bound to the same polypeptide chain. In Figure S5, the MeHydA amino acid sequence is aligned with that of *C. pasteurianum*, demonstrating 40 % sequence identity. CpHydA has a long N-terminal stretch, absent in MeHydA, which chelates one [2Fe-2S] and one [4Fe-4S] cluster. Based on this alignment and the three-dimensional structure of CpHydA, one can easily identify the cysteines of MeHydA involved in binding the H-cluster (C highlighted in yellow) and the ancillary [FeS] clusters (C highlighted in green and magenta respectively). Such an assignment requires a future confirmation by site-directed mutagenesis.

3.2 Synthetic maturation

Applying the methodology recently reported [26], we next reacted FeS-MeHydA with an excess of the synthetically prepared diiron biomimetic complex $[Fe_2(adt)(CO)_4(CN)_2]^{2-}$ for one hour anaerobically and then purified the protein by desalting (NAP 10) in order to remove the excess of the mimic. Evidence for maturation of the protein, thus named holo-MeHydA, was obtained by enzymatic assay. Using a standard assay based on the reduction of protons by dithionite/methyl viologen and quantification of dihydrogen by gas chromatography, we showed that holo-MeHydA was highly active. A specific hydrogenase activity of 600 ± 50 μmol $H_2.mg^{-1}.min^{-1}$, that corresponds to a TOF of 550 turnovers per second (MW 54.5 kDa), was obtained for holo-MeHydA. In the presence of an excess of the mimic, the measured hydrogenase activity was lower by ~33% (400 ± 50 $\mu mol.mg^{-1}.min^{-1}$), possibly because of release of CO, an enzyme inhibitor, from the mimic in excess. An activity of 400 $\mu mol\ H_2.mg^{-1}.min^{-1}$, for native MeHydA has been reported [**34**].

3.3 FTIR and EPR spectroscopic characterization of the active site

In order to confirm that the H-cluster has been assembled correctly but also to provide a full characterization of active *M. elsdenii* HydA, we used Fourier Transform Infrared (FTIR) spectroscopy for characterization (Figure 3A, Table 1). FTIR is appropriate for identifying the CO (1800-2020 cm^{-1}) and CN (2040-2100 cm^{-1}) vibrations associated with the CO and CN^- ligands present in the 2Fe-subcluster [18]. These signals can be clearly distinguished from those of the $[Fe_2(adt)(CO)_4(CN)_2]^{2-}$ complex in solution which are much broader (Figure 3A, top) [27]. The narrow CO and CN FTIR bands of the H-cluster allow differentiating between the various

states usually coexisting in hydrogenase preparations. The paramagnetic states of the H-cluster (as well as the $[4Fe\text{-}4S]^{1+}$ clusters in the unmaturated enzyme) were also studied using EPR.

In the as-isolated sample (after chemical maturation), a mixture of mainly H_{ox} and H_{ox}-CO states, all expectedly containing a CO bridge revealed by the 1803/1804 cm^{-1} feature, is observed. Under synthetic maturation, the supernumerary CO is released from the complex $[Fe_2(adt)(CO)_4(CN)_2]^{2-}$resulting in a substantial amount of the H_{ox}-CO state. This signal is also often present in [FeFe]-hydrogenase preparations due to the so-called ‘‘cannibalization process’’ in which the CO ligands, from light- or oxygen-damaged H-clusters, are released and captured by H-clusters that are still intact [30,38,51]. Additional CO is “leaking” from the excess binuclear complex present in the maturation buffer further increasing the H_{ox}-CO population (Figure 3A). To obtain a pure CO inhibited state, the sample was flushed for 20 minutes with CO gas. The FTIR spectrum is shown in Figure 3A and is in good agreement with previously obtained data from different [FeFe]-hydrogenases (Table 1). The H_{ox}-CO state can be converted to the H_{ox} state by flushing the sample with argon gas for 1 hour. The FTIR spectrum presented in Figure 4A again shows the typical signals of the H_{ox} state (see Table 1) with a small contamination of H_{ox}-CO and H_{red}. Finally, upon reduction, H_{ox} is converted into the H_{red} state, It turns out that MeHydA cannot be fully reduced by H_2 flushing, thus additional sodium dithionite treatment (5-10 mM) was needed (see Figure S4). The FTIR signature of MeHydA-H_{red} and DdH-H_{red} are very similar but different from Cr-HydA1-H_{red} which still contains a bridging CO ligand. Instead the H_{red} state in bacterial [FeFe] hydrogenases has an FTIR spectrum resembling that of *Cr*HydA1-H_{sred} (see Table 1). It should be noted that before the present work, an FTIR spectrum of HydA isolated from *M. elsdenii* was reported [52]. However, while some (not all)

CO vibrational features characteristic of H_{ox} and H_{red} were present, no CN vibrations could be observed. This raises uncertainties regarding the relevance of these data.

Table 1. Collection of FTIR vibrations associated with the CO and CN ligands present in the [2Fe] subcluster for different HydAs.

Organism	Species	Fe-CN	Fe-CO	Fe-CO-Fe	Ref
M. elsdenii	**H_{ox}**	**2087, 2079**	**1964, 1937**	**1803**	**This work**
D. desulfuricans	**H_{ox}**	**2093, 2079**	**1965, 1940**	**1802**	**[38]**
C. pasteurianum	**H_{ox}**	**2086, 2072**	**1971, 1948**	**1802**	**[53]**
C. reinhardtii	**H_{ox}**	**2088, 2072**	**1964, 1940**	**1800**	**[40]**
C. acetobutylicum	**H_{ox}**	**2082, 2070**	**1969, 1946**	**1801**	**[54]**
M. elsdenii	**H_{ox}-CO**	**2090**	**2013, 1969, 1955**	**1804**	**This work**
D. desulfuricans	**H_{ox}-CO**	**2096, 2088**	**2016, 1971,1963**	**1810**	**[38]**
C. pasteurianum	**H_{ox}-CO**	**2095, 2077**	**2017, 1974,1971**	**1810**	**[53]**
C. reinhardtii	**H_{ox}-CO**	**2092, 2084**	**2013, 1970,1964**	**1810**	**[40]**
C. acetobutylicum	**H_{ox}-CO**	**2090, 2075**	**2015, 1973, 1967**	**1806**	**[54]**
M. elsdenii	**H_{red}**	**2069, 2041**	**1956, 1916, 1891**		**This work**
D. desulfuricans	**H_{red}**	**2079, 2041**	**1965, 1916,1894**		**[38]**
C. acetobutylicum	**H_{red}**	**2053, 2040**	**1899**		**[54]**
C. reinhardtii	**H_{red}**	**2083, 2070**	**1935, 1891**	**1793**	**[40]**
C. reinhardtii	**H_{sred}**	**2070, 2026**	**1954, 1919, 1882**		**[39,40]**

Figure 3B shows the EPR spectra of the oxidized forms described above. The EPR spectrum of the pure H_{ox}-CO state is characterized by a nearly axial signal originating from the low spin mixed-valence configuration of the 2Fe-subcluster Fe(I)Fe(II) while the [4Fe–4S] cluster is in the oxidized 2+ state. Although the redox states of H_{ox} and H_{ox}-CO are the same, the EPR signal originating from the 2Fe-subcluster in H_{ox} is rhombic. Only the rhombic signal has been reported before in the literature [55]. Finally, the H_{red} state is EPR silent in agreement with the 2Fe-subcluster being in the S=0 Fe(I)Fe(I) state.

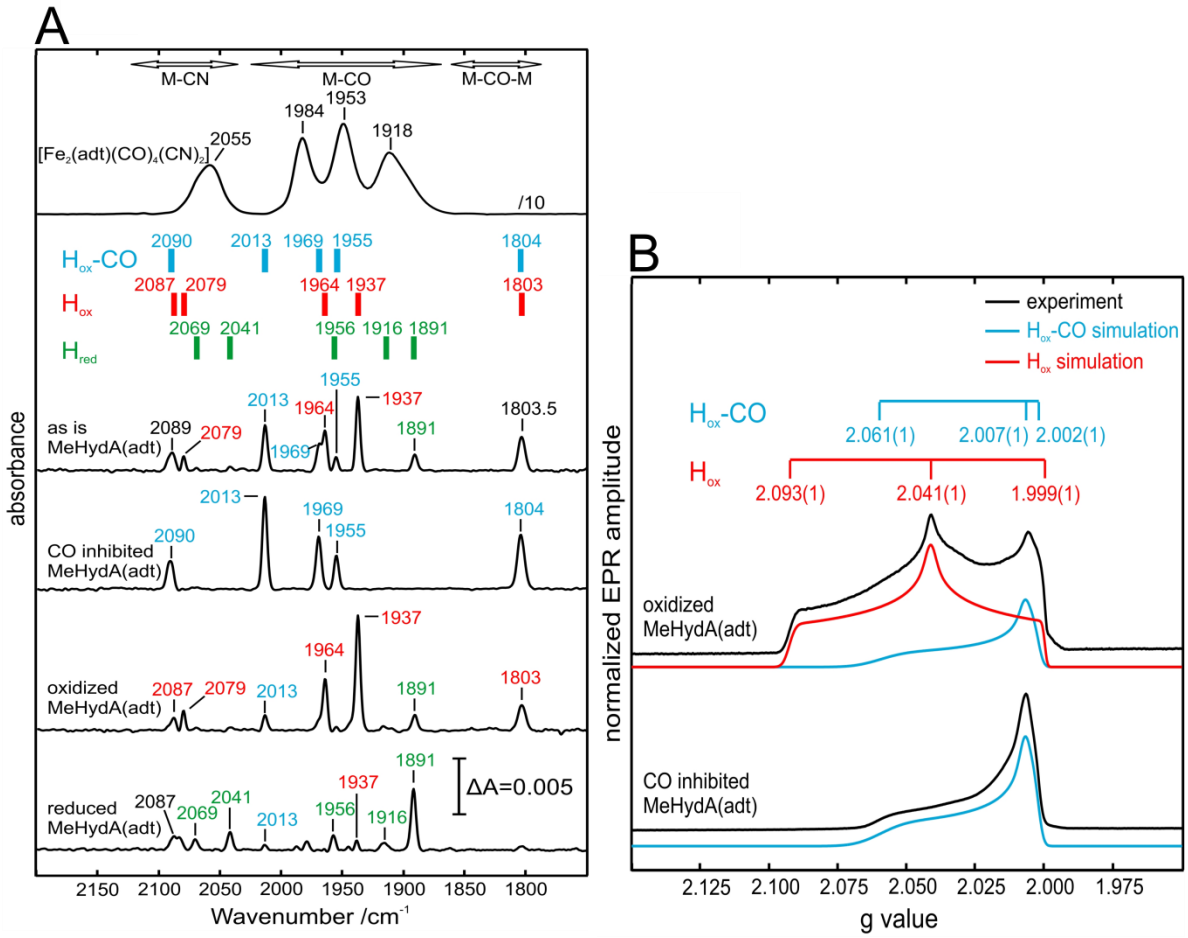

Figure 3. EPR and FTIR spectra of chemically maturated MeHydA. **A**)FTIR spectra of $[Fe_2(adt)(CO)_4(CN)_2]^{2-}$, holo-MeHydA as isolated, H_{ox}, H_{ox}-CO and H_{red} states in 100 mM potassium phosphate pH 6.8. **B**) Q-band FID-detected EPR-spectra (T = 10K) of 0.5 mM holo-MeHydA in the H_{ox}-CO and H_{ox} states in 100 mM potassium phosphate pH 6.8 and their simulations. Information about FTIR and EPR signal positions for each redox state is presented at the top of the panels (A, B) and in Table 1 and Table 2, respectively.

The different states of the H-cluster H_{ox}-CO, H_{ox}, and H_{red} in MeHydA have thus been prepared following procedures similar to those reported for other bacterial [FeFe] hydrogenases [38,56]. The spectral features of the H-cluster in these three states can be compared with those found for HydA from the organisms *D. desulfuricans*, *C. pasteurianum*, and *C. reinhardtii* (Table 1 and 2). It turns out that the FTIR bands and EPR g-values of H_{ox} and H_{ox}-CO are very similar in all species. Only the g_1-value of H_{ox}-CO shows some variability where *M. elsdenii* is closest to *D. desulfuricans*. Also the FTIR signature of the EPR silent H_{red} state of MeHydA is

very similar to that of the other bacterial [FeFe]-hydrogenases. While for *C. reinhardtii* (lacking the extra clusters) the (semi) bridging CO ligand is still present, it is a terminal CO in hydrogenases from *M. elsdenii* and the other bacterial species. On the other hand, the doubly reduced state H_{sred} observed in algae (*Cr*) is not stable and undetectable in bacterial [FeFe]-hydrogenases.

Table 2. Collection of EPR g values of the H cluster for HydA in different species.

Organism	Species	g1	g2	g3	Ref
M. elsdenii	H_{ox}	**2.093**	**2.041**	**1.999**	**This work**
D. desulfuricans	H_{ox}	**2.100**	**2.040**	**1.998**	**[51]**
C. pasteurianum	H_{ox}	**2.097**	**2.039**	**1.999**	**[57]**
C. reinhardtii	H_{ox}	**2.104**	**2.042**	**1.998**	**[26]**
C. acetobutylicum	H_{ox}	**2.089**	**2.036**	**1.995**	**[54]**
M. elsdenii	H_{ox}-CO	**2.061**	**2.007**	**2.002**	**This work**
D. desulfuricans	H_{ox}-CO	**2.065**	**2.007**	**2.001**	**[51]**
C. pasteurianum	H_{ox}-CO	**2.072**	**2.006**	**2.006**	**[57]**
C. reinhardtii	H_{ox}-CO	**2.054**	**2.009**	**2.009**	**[26]**
C. acetobutylicum	H_{ox}-CO	**2.075**	**2.009**	**2.009**	**[54]**
C. reinhardtii	H_{sred}	**2.073**	**1.935**	**1.880**	**[26]**
D. desulfuricans	H_{trans}	**2.060**	**1.960**	**1.890**	**[51]**

4. CONCLUSIONS

We present a very efficient method for producing an [FeFe]-hydrogenase by heterologous expression in E. *coli* of the structural gene, aerobic purification in two steps, chemical reconstitution of [FeS] clusters and subsequent chemical maturation with a synthetic organometallic active site mimic. Straightforward high-yield aerobic purification affords the apo-enzyme without any metallic cofactors. Subsequent reconstitution of the (oxygen sensitive) [4Fe-4S] clusters is carried out chemically from iron salt and sulfide under anaerobic conditions. We show in the case of MeHydA that this is efficient even for the case of a protein containing three [4Fe-4S] clusters. Treatment with the $[Fe_2(adt)(CO)_4(CN)_2]^{2-}$ mimic complex completes

the activation process, as it generates a fully assembled catalytically competent H-cluster – including the 2Fe-subcluster. In the case of MeHydA this procedure is highly efficient since we obtain for this enzyme a high specific activity (600 μmol H_2.mg^{-1}.min^{-1}). FTIR and EPR spectroscopic characterization confirms that the redox states of the MeHydA enzyme are very similar to the bacterial [FeFe] hydrogenases from *D*. *desulfuricans* and *C*. *pasteurianum*. With this proof of concept we hope that this methodology can be applied to other hydrogenases from other living organisms for large scale production of an active enzyme. It is one of the many possible applications of the discovery that simple chemical reactants, iron and sulfide as well as $[Fe_2(adt)(CO)_4(CN)_2]^{2-}$, can fully replace the complex metallocofactor biosynthetic machineries within the same hydrogenase, the [FeS] cluster assembly machinery and the HydEFG machinery, respectively.

Appendix A. Supplementary material

Aerobic protein purification (Figure S1), *in vitro* [4Fe-4S] clusters reconstitution (Figure S2), anaerobic purification of FeS-MeHydA (Figure S3), progressive reduction of maturated MeHydA(adt) observed by FTIR (Figure S4), sequence alignment of MeHydA with CpHydA.

Appendix B. Author Contributions

The manuscript was written through contributions of all authors. All authors have given approval to the final version of the manuscript.

ACKNOWLEDGMENT

We thank Dr. Simon Arragain for useful discussion and Bruno Faivre for excellent technical assistance on MeHydA preparation. We acknowledge financial support from the French National

Research Agency (Labex programs ARCANE, ANR-11-LABX-0003-01 and DYNAMO, ANR-11-LABX-0011), from Fondation de l'Orangerie for individual Philanthropy and its donors, and from the Max Planck Society.

REFERENCES

[1] W. Lubitz, H. Ogata, O. Rüdiger, E. Reijerse, Hydrogenases, Chem. Rev., 114 (2014) 4081–4148.

[2] T. Lautier, P. Ezanno, C. Baffert, V. Fourmond, L. Cournac, J.C. Fontecilla-Camps, P. Soucaille, P. Bertrand, I. Meynial-Salles, C. Léger, The quest for a functional substrate access tunnel in FeFe hydrogenase, Faraday Discuss, 148 (2011) 385–407.

[3] D.W. Mulder, E.M. Shepard, J.E. Meuser, N. Joshi, P.W. King, M.C. Posewitz, J.B. Broderick, J.W. Peters, Insights into [FeFe]-Hydrogenase Structure, Mechanism, and Maturation, Structure, 19 (2011) 1038–1052.

[4] V. Artero, G. Berggren, M. Atta, G. Caserta, S. Roy, L. Pecqueur, M. Fontecave, From Enzyme Maturation to Synthetic Chemistry: The Case of Hydrogenases, Acc. Chem. Res., 48 (2015) 2380–2387.

[5] T.W. Woolerton, S. Sheard, Y.S. Chaudhary, F.A. Armstrong, Enzymes and bio-inspired electrocatalysts in solar fuel devices, Energy Environ. Sci., 5 (2012) 7470–7490.

[6] J.A. Cracknell, K.A. Vincent, F.A. Armstrong, Enzymes as working or inspirational electrocatalysts for fuel cells and electrolysis, Chem. Rev., 108 (2008) 2439–2461.

[7] F.A. Armstrong, N.A. Belsey, J.A. Cracknell, G. Goldet, A. Parkin, E. Reisner, K.A. Vincent, A.F. Wait, Dynamic electrochemical investigations of hydrogen oxidation and production by enzymes and implications for future technology, Chem. Soc. Rev., 38 (2009) 36–51.

[8] G. Caserta, S. Roy, M. Atta, V. Artero, M. Fontecave, Artificial hydrogenases: biohybrid and supramolecular systems for catalytic hydrogen production or uptake, Curr. Opin. Chem. Biol., 25 (2015) 36–47.

[9] T. Noji, M. Kondo, T. Jin, T. Yazawa, H. Osuka, Y. Higuchi, M. Nango, S. Itoh, T. Dewa, Light-Driven Hydrogen Production by Hydrogenases and a Ru-Complex inside a Nanoporous Glass Plate under Aerobic External Conditions, J. Phys. Chem. Lett., 5 (2014) 2402–2407.

[10] V. Fourmond, C. Greco, K. Sybirna, C. Baffert, P.-H. Wang, P. Ezanno, M. Montefiori, M. Bruschi, I. Meynial-Salles, P. Soucaille, J. Blumberger, H. Bottin, L. De Gioia, C. Léger, The oxidative inactivation of FeFe hydrogenase reveals the flexibility of the H-cluster, Nat. Chem., 6 (2014) 336–342.

[11] D.W. Wakerley, E. Reisner, Oxygen-tolerant proton reduction catalysis: much O_2 about nothing?, Energy Env. Sci, 8 (2015) 2283–2295.

[12] M.L. Ghirardi, Implementation of photobiological H2 production: the O 2 sensitivity of hydrogenases, Photosynth. Res., 125 (2015) 383–393.

[13] C. Orain, L. Saujet, C. Gauquelin, P. Soucaille, I. Meynial-Salles, C. Baffert, V. Fourmond, H. Bottin, C. Léger, Electrochemical Measurements of the Kinetics of Inhibition of Two FeFe Hydrogenases by O_2 Demonstrate That the Reaction Is Partly Reversible, J. Am. Chem. Soc., 137 (2015) 12580–12587.

[14] A. Kubas, D. De Sancho, R.B. Best, J. Blumberger, Aerobic damage to [FeFe]-hydrogenases: activation barriers for the chemical attachment of O2, Angew. Chem. Int. Ed., 53 (2014) 4081–4084.

[15] A.A. Oughli, F. Conzuelo, M. Winkler, T. Happe, W. Lubitz, W. Schuhmann, O. Rüdiger, N. Plumeré, A Redox Hydrogel Protects the O_2 -Sensitive [FeFe]-Hydrogenase from *Chlamydomonas reinhardtii* from Oxidative Damage, Angew. Chem. Int. Ed., 54 (2015) 12329–12333.

[16] T.R. Simmons, G. Berggren, M. Bacchi, M. Fontecave, V. Artero, Mimicking hydrogenases: From biomimetics to artificial enzymes, Coord. Chem. Rev., 270 (2014) 127–150.

[17] C. Tard, C.J. Pickett, Structural and Functional Analogues of the Active Sites of the [Fe]-, [NiFe]-, and [FeFe]-Hydrogenases, Chem. Rev., 109 (2009) 2245–2274.

[18] Y. Nicolet, A.L. de Lacey, X. Vernède, V.M. Fernandez, E.C. Hatchikian, J.C. Fontecilla-Camps, Crystallographic and FTIR spectroscopic evidence of changes in Fe coordination upon reduction of the active site of the Fe-only hydrogenase from Desulfovibrio desulfuricans, J. Am. Chem. Soc., 123 (2001) 1596–1601.

[19] J.W. Peters, W.N. Lanzilotta, B.J. Lemon, L.C. Seefeldt, X-ray crystal structure of the Fe-only hydrogenase (CpI) from Clostridium pasteurianum to 18 angstrom resolution, Science, 282 (1998) 1853–1858.
[20] A.S. Pandey, T.V. Harris, L.J. Giles, J.W. Peters, R.K. Szilagyi, Dithiomethylether as a ligand in the hydrogenase h-cluster, J. Am. Chem. Soc., 130 (2008) 4533–4540.
[21] Y. Nicolet, C. Piras, P. Legrand, C.E. Hatchikian, J.C. Fontecilla-Camps, Desulfovibrio desulfuricans iron hydrogenase: the structure shows unusual coordination to an active site Fe binuclear center, Struct. Lond. Engl. 1993, 7 (1999) 13–23.
[22] D.W. Mulder, E.S. Boyd, R. Sarma, R.K. Lange, J.A. Endrizzi, J.B. Broderick, J.W. Peters, Stepwise [FeFe]-hydrogenase H-cluster assembly revealed in the structure of HydA(DeltaEFG), Nature, 465 (2010) 248–251.
[23] E.M. Shepard, F. Mus, J.N. Betz, A.S. Byer, B.R. Duffus, J.W. Peters, J.B. Broderick, [FeFe]-Hydrogenase Maturation, Biochemistry, 53 (2014) 4090–4104.
[24] D.L.M. Suess, I. Bürstel, L. De La Paz, J.M. Kuchenreuther, C.C. Pham, S.P. Cramer, J.R. Swartz, R.D. Britt, Cysteine as a ligand platform in the biosynthesis of the FeFe hydrogenase H cluster, Proc. Natl. Acad. Sci. U. S. A., 112 (2015) 11455–11460.
[25] J.W. Peters, G.J. Schut, E.S. Boyd, D.W. Mulder, E.M. Shepard, J.B. Broderick, P.W. King, M.W.W. Adams, [FeFe]- and [NiFe]-hydrogenase diversity, mechanism, and maturation, Biochim. Biophys. Acta, 1853 (2015) 1350–1369.
[26] J. Esselborn, C. Lambertz, A. Adamska-Venkatesh, T. Simmons, G. Berggren, J. Noth, J. Siebel, A. Hemschemeier, V. Artero, E. Reijerse, M. Fontecave, W. Lubitz, T. Happe, Spontaneous activation of [FeFe]-hydrogenases by an inorganic [2Fe] active site mimic, Nat. Chem. Biol., 9 (2013) 607–609.
[27] G. Berggren, A. Adamska, C. Lambertz, T.R. Simmons, J. Esselborn, M. Atta, S. Gambarelli, J.-M. Mouesca, E. Reijerse, W. Lubitz, T. Happe, V. Artero, M. Fontecave, Biomimetic assembly and activation of [FeFe]-hydrogenases, Nature, 499 (2013) 66–69.
[28] J. Esselborn, N. Muraki, K. Klein, V. Engelbrecht, N. Metzler-Nolte, U.-P. Apfel, E. Hofmann, G. Kurisu, T. Happe, A structural view of synthetic cofactor integration into [FeFe]-hydrogenases, Chem Sci, 7 (2016) 959–968.
[29] A. Adamska-Venkatesh, T.R. Simmons, J.F. Siebel, V. Artero, M. Fontecave, E. Reijerse, W. Lubitz, Artificially maturated [FeFe] hydrogenase from Chlamydomonas reinhardtii: a HYSCORE and ENDOR study of a non-natural H-cluster, Phys. Chem. Chem. Phys., 17 (2015) 5421–5430.
[30] A. Adamska-Venkatesh, D. Krawietz, J. Siebel, K. Weber, T. Happe, E. Reijerse, W. Lubitz, New Redox States Observed in [FeFe] Hydrogenases Reveal Redox Coupling Within the H-Cluster, J. Am. Chem. Soc., 136 (2014) 11339–11346.
[31] A. Adamska-Venkatesh, S. Roy, J.F. Siebel, T.R. Simmons, M. Fontecave, V. Artero, E. Reijerse, W. Lubitz, Spectroscopic Characterization of the Bridging Amine in the Active Site of [FeFe] Hydrogenase Using Isotopologues of the H-Cluster, J. Am. Chem. Soc., 137 (2015) 12744–12747.
[32] R. Gilbert-Wilson, J.F. Siebel, A. Adamska-Venkatesh, C.C. Pham, E. Reijerse, H. Wang, S.P. Cramer, W. Lubitz, T.B. Rauchfuss, Spectroscopic Investigations of [FeFe] Hydrogenase Maturated with [(57)Fe2(adt)(CN)2(CO)4](2-), J. Am. Chem. Soc., 137 (2015) 8998–9005.
[33] J.F. Siebel, A. Adamska-Venkatesh, K. Weber, S. Rumpel, E. Reijerse, W. Lubitz, Hybrid [FeFe]-hydrogenases with modified active sites show remarkable residual enzymatic activity, Biochemistry, 54 (2015) 1474–1483.
[34] M. Filipiak, W.R. Hagen, C. Veeger, Hydrodynamic, structural and magnetic properties of Megasphaera elsdenii Fe hydrogenase reinvestigated, Eur. J. Biochem., 185 (1989) 547–553.
[35] C. Van Dijk, S.G. Mayhew, H.J. Grande, C. Veeger, Purification and properties of hydrogenase from Megasphaera elsdenii, Eur. J. Biochem., 102 (1979) 317–330.

[36] C. Van Dijk, H.J. Grande, S.G. Mayhew, C. Veeger, Properties of the hydrogenase of Megasphaera elsdenii, Eur. J. Biochem., 107 (1980) 251–261.
[37] C. Van Dijk, C. VEEGER, The effects of pH and redox potential on the hydrogen production activity of the hydrogenase from Megasphaera elsdenii, Eur. J. Biochem., 114 (1981) 209–219.
[38] W. Roseboom, A.L. De Lacey, V.M. Fernandez, E.C. Hatchikian, S.P.J. Albracht, The active site of the [FeFe]-hydrogenase from Desulfovibrio desulfuricans II Redox properties, light sensitivity and CO-ligand exchange as observed by infrared spectroscopy, J. Biol. Inorg. Chem. , 11 (2006) 102–118.
[39] A. Adamska, A. Silakov, C. Lambertz, O. Rüdiger, T. Happe, E. Reijerse, W. Lubitz, Identification and Characterization of the "Super-Reduced" State of the H-Cluster in [FeFe] Hydrogenase: A New Building Block for the Catalytic Cycle?, Angew. Chem.-Int. Ed., 51 (2012) 11458–11462.
[40] A. Silakov, C. Kamp, E. Reijerse, T. Happe, W. Lubitz, Spectroelectrochemical Characterization of the Active Site of the [FeFe] Hydrogenase HydA1 from Chlamydomonas reinhardtii, Biochemistry, 48 (2009) 7780–7786.
[41] M. Atta, J. Meyer, Characterization of the gene encoding the [Fe]-hydrogenase from Megasphaera elsdenii, Biochim. Biophys. Acta BBA - Protein Struct. Mol. Enzymol., 1476 (2000) 368–371.
[42] H. Zhao, P.H. Brown, P. Schuck, On the distribution of protein refractive index increments, Biophys. J., 100 (2011) 2309–2317.
[43] L. Loiseau, S. Ollagnier-de Choudens, D. Lascoux, E. Forest, M. Fontecave, F. Barras, Analysis of the heteromeric CsdA-CsdE cysteine desulfurase, assisting Fe-S cluster biogenesis in Escherichia coli, J. Biol. Chem., 280 (2005) 26760–26769.
[44] W.W. Fish, Rapid colorimetric micromethod for the quantitation of complexed iron in biological samples, Methods Enzymol., 158 (1988) 357–364.
[45] H. Beinert, Semi-micro methods for analysis of labile sulfide and of labile sulfide plus sulfane sulfur in unusually stable iron-sulfur proteins, Anal. Biochem., 131 (1983) 373–378.
[46] H. Li, T.B. Rauchfuss, Iron carbonyl sulfides, formaldehyde, and amines condense to give the proposed azadithiolate cofactor of the Fe-only hydrogenases, J. Am. Chem. Soc., 124 (2002) 726–727.
[47] E. Reijerse, F. Lendzian, R. Isaacson, W. Lubitz, A tunable general purpose Q-band resonator for CW and pulse EPR/ENDOR experiments with large sample access and optical excitation, J. Magn. Reson., 214 (2012) 237–243.
[48] S. Stoll, A. Schweiger, EasySpin, a comprehensive software package for spectral simulation and analysis in EPR, J. Magn. Reson., 178 (2006) 42–55.
[49] L.E. Netto, E.R. Stadtman, The iron-catalyzed oxidation of dithiothreitol is a biphasic process: hydrogen peroxide is involved in the initiation of a free radical chain of reactions, Arch. Biochem. Biophys., 333 (1996) 233–242.
[50] G. Voordouw, W.R. Hagen, K.M. Krüse-Wolters, A. van Berkel-Arts, C. Veeger, Purification and characterization of Desulfovibrio vulgaris (Hildenborough) hydrogenase expressed in Escherichia coli, Eur. J. Biochem., 162 (1987) 31–36.
[51] S.P.J. Albracht, W. Roseboom, E.C. Hatchikian, The active site of the [FeFe]-hydrogenase from Desulfovibrio desulfuricans I Light sensitivity and magnetic hyperfine interactions as observed by electron paramagnetic resonance, J. Biol. Inorg. Chem., 11 (2006) 88–101.
[52] T.M. Van der Spek, A.F. Arendsen, R.P. Happe, S. Yun, K.A. Bagley, D.J. Stufkens, W.R. Hagen, S.P. Albracht, Similarities in the architecture of the active sites of Ni-hydrogenases and Fe-hydrogenases detected by means of infrared spectroscopy, Eur. J. Biochem., 237 (1996) 629–634.
[53] Z. Chen, B.J. Lemon, S. Huang, D.J. Swartz, J.W. Peters, K.A. Bagley, Infrared studies of the CO-inhibited form of the Fe-only hydrogenase from Clostridium pasteurianum I: examination of its light sensitivity at cryogenic temperatures, Biochemistry, 41 (2002) 2036–2043.

[54] S. Morra, S. Maurelli, M. Chiesa, D.W. Mulder, M.W. Ratzloff, E. Giamello, P.W. King, G. Gilardi, F. Valetti, The effect of a C298D mutation in CaHydA [FeFe]-hydrogenase: Insights into the protein-metal cluster interaction by EPR and FTIR spectroscopic investigation, Biochim. Biophys. Acta BBA - Bioenerg., 1857 (2016) 98–106.
[55] P.J. van Dam, E.J. Reijerse, W.R. Hagen, Identification of a putative histidine base and of a non-protein nitrogen ligand in the active site of Fe-hydrogenases by one-dimensional and two-dimensional electron spin-echo envelope-modulation spectroscopy, Eur. J. Biochem., 248 (1997) 355–361.
[56] D.W. Mulder, M.W. Ratzloff, E.M. Shepard, A.S. Byer, S.M. Noone, J.W. Peters, J.B. Broderick, P.W. King, EPR and FTIR Analysis of the Mechanism of H_2 Activation by [FeFe]-Hydrogenase HydA1 from Chlamydomonas reinhardtii, J. Am. Chem. Soc., 135 (2013) 6921–6929.
[57] B. Bennett, B.J. Lemon, J.W. Peters, Reversible carbon monoxide binding and inhibition at the active site of the Fe-only hydrogenase, Biochemistry, 39 (2000) 7455–7460.

Graphical abstract